
SELECTED ENGINEERING PROBLEMS

NUMBER 4

INSTITUTE OF ENGINEERING PROCESSES AUTOMATION
AND INTEGRATED MANUFACTURING SYSTEMS

Michał ZUBA, Rafał RZAŚIŃSKI*

Institute of Engineering Processes Automation and Integrated Manufacturing Systems,
Faculty of Mechanical Engineering, Silesian University of Technology, Gliwice, Poland

*rafal.rzasinski@polsl.pl

A CONCEPT OF AERODYNAMICALLY OPTIMIZED ELECTRIC CAR BODYWORK

Abstract: The article presents the process of selecting an optimal concept of an electric car bodywork according to the criterion of minimum aerodynamic drag. It also presents design and construction assumptions, the field of possible solutions and aerodynamic simulation results. Based on the performed analyzes, an optimal design solution was selected and graphical results of simulations for the best solution were presented.

1. Introduction

Due to the widespread ecological trend related to the environmental performance of vehicles, the aim is to achieve maximum performance with minimum consumption of energy supplied. One of the ways of attaining this goal is to create a bodywork characterized by a minimum value of aerodynamic drag. Every year the produced vehicles have better aerodynamic properties, but it is still necessary to search for better and more efficient solutions.

2. Bodywork

In the process of devising, the following design and construction assumptions were adopted [1]:

- The total height of the vehicle: 1000-1300 [mm],
- The total width of bodywork (excluding rear view mirrors): 1200-1300 [mm],
- The total length of the vehicle: 2200-3500 [mm],
- The track width of the front axle: ≥ 1000 [mm] (between the midpoints where the tyres touch the ground),
- The track width of the rear axle: ≥ 800 [mm] (between the midpoints where the tyres touch the ground),
- The wheelbase: ≥ 1200 [mm],
- The driver's compartment: height: ≥ 880 [mm], width: ≥ 700 [mm],
- The ground clearance: ≥ 100 [mm],

Based on the design and construction assumptions as well as information about aerodynamics of vehicles, eight concepts of bodywork were modeled in a CAD environment in the Siemens NX 8.5 (Fig. 1). In the process of virtual models designing the so-called radical method, based on simple shapes with a low value of aerodynamic drag, was selected. Having regard to minimizing the vehicle weight, it is assumed that the bodywork will be made from composite materials, therefore all of the proposed concepts were modeled as self-supporting bodywork (monocoque) [9]. During the modeling process, efforts were undertaken to preserve a minimal value of the face area, bearing in mind its negative effect on air resistance increase. For all the concepts it has been assumed that the cars are equipped with full wheels and internally assembled rear view mirrors, which is most favorable from the aerodynamic point of view.

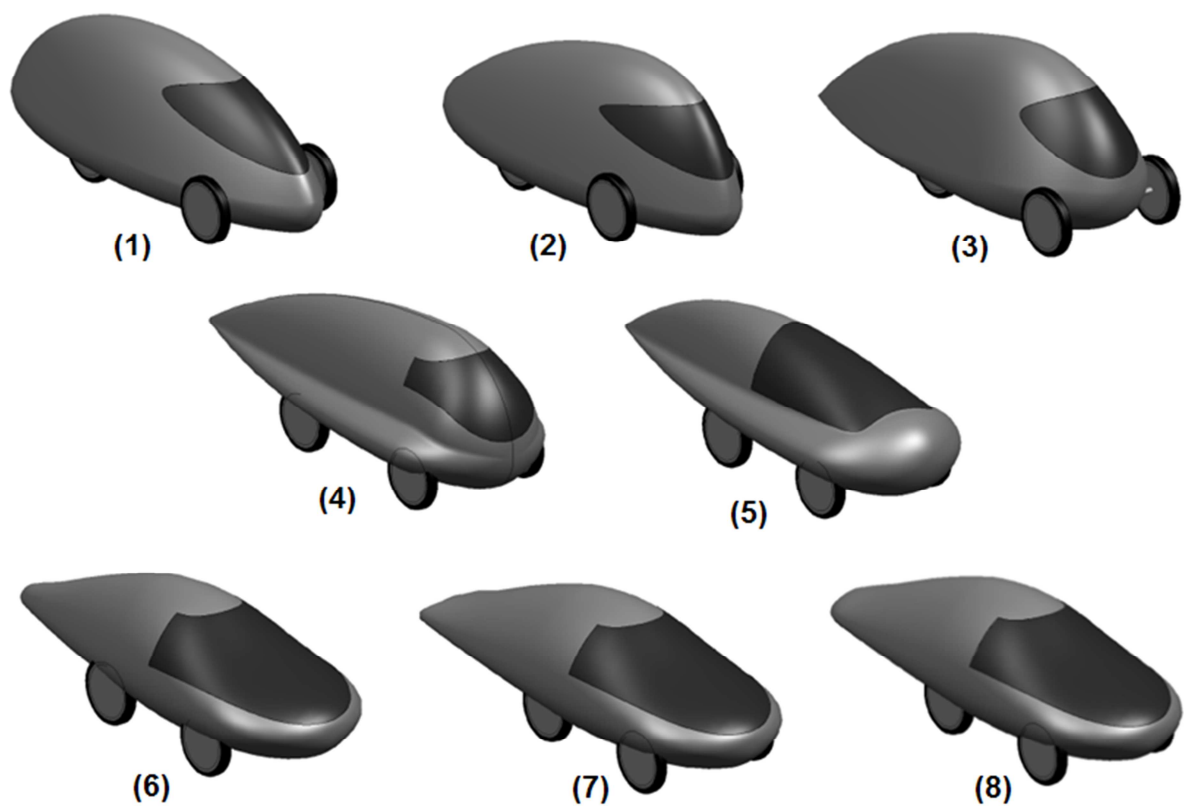


Fig.1. The proposed field of possible solutions for the electric car's bodywork

3. Numerical simulation

In order to achieve the task, numerical methods were applied. Due to the complicated form of design concepts, the computational models required a large amount of data to be analyzed. This significantly increased the time of preparing the model (determination of the finite element mesh and boundary conditions) and, in consequence, the time required to obtain the results. Every small change entailed recalculating the data and even generating a new mesh. The obtained results reflect the aerodynamic flows but it should be noted that the most accurate data on vehicle aerodynamics is still obtained in aerodynamic tunnel tests.

In aerodynamic simulations the SST turbulence model was used for all the proposed bodywork concepts and the method applied was based on the CSG technique. During the simulation, the air flow rate was set at 9 [m/s] (32.4 [km/h]).

In order to choose the best method of calculation, simulations for the selected 3 bodywork concepts were conducted by two methods. The calculation based on the method using two models took ca.12-24h and as a result thereof were generated reports with abstract resistance values. The calculation time based on the method employing the CSG technique reached ca 3-5h for a single simulation and the results of reports had real values. In addition, it should be noted that the calculations were performed on a PC with eight-core processor 3.4 GHz and 8 GB of RAM.

4. Summary of simulation results and selection of the optimal concept

When choosing the best bodywork concept, the optimization straight with single objective was used, due to the minimization of total aerodynamic drag forces:

$$F_{ON} \rightarrow F_{ON \min} \quad (1)$$

In order to perform optimization, the results of aerodynamic drag reports generated by the program Siemens NX 8.5 were collected in Tab. 1. Additionally, the statement contains the face area and its product with the drag coefficient c_x , which indicates the body's general aerodynamic excellence. In each category the extremely positive results have been marked with green color and extremely negative ones have been highlighted in red.

Tab.1. Summary of the results of aerodynamic calculations performed in the Siemens NX 8.5

Concept	c_x [-]	A [m ²]	$c_x \cdot A$ [m ²]	F _P [N]	F _N [N]	F _{ON} [N]
1	0.212613	0.959349	0.203970	9.97077	-3.60263	10.60166
2	0.176384	0.988488	0.174353	8.52295	2.52635	8.88949
3	0.201707	1.049995	0.211791	10.35310	2.19488	10.58320
4	0.207182	0.964264	0.199778	9.76580	-2.40740	10.05815
5	0.225169	0.840235	0.189195	9.24850	-1.98676	9.45949
6	0.170008	0.968411	0.164638	8.04805	-2.88323	8.54893
7	0.167847	0.988214	0.165869	8.10820	-1.96932	8.34393
8	0.178090	0.989554	0.176230	8.61470	-2.66690	9.01806

The above table (Tab. 1) shows that the most favorable value of the drag coefficient c_x was recorded for the seventh concept, closely followed by the sixth one with a slightly worse result, and next, by the second and eighth solution. The worst aerodynamic drag coefficient was noted for the fifth body. In most of the concepts the face surface area ranged between 0.95-0.99 [m²]. The highest value of the face area was recorded for the third concept, which, combined with a weak drag coefficient, generates the worst product of the overall excellence of the aerodynamic body. The smallest face area was observed for the fifth concept, characterized by the worst drag coefficient, which gives an average result of the product of

the overall aerodynamic excellence compared to other solutions. The best value of this product was noted for the sixth concept, whereas the seventh one was a slightly worse solution. As indicated by the statement, the product of aerodynamic excellence has a direct impact on the value of air resistance force - the highest value of air resistance $F_p = 10.35310[\text{N}]$ was recorded for the third concept and the smallest $F_p = 8.04805[\text{N}]$ – for the sixth solution. Little worse result (not exceeding the value of $8.5[\text{N}]$) was noted for the seventh and second concept. Total aerodynamic resistance also consists of lift force, which reached the lowest value in the seventh concept and the highest in the first one. A minus sign before the value of the lift force means that it is directed to the ground, i.e. it is an aerodynamic pressing force. A comparison of the total aerodynamic drag shows that the first concept is the worst solution (F_{ONmax}) in terms of aerodynamics. The most optimal concept from the point of view of the aerodynamic criterion (F_{ONmin}) is the seventh solution.

5. Graphical representation of the results

As a result of the simulation, the seventh concept reached drag coefficient $c_x = 0.167847[-]$ and air resistance $F_p = 8.10820[\text{N}]$. The pressure exerted on the surface of the body (Fig. 2) reaches the highest values at a relatively small area of the vehicle "nose" and on the front part of the wheels. The highest value is on the "nose" of the vehicle, reaching $58.20[\text{Pa}]$. This value results from the high air pressure ahead of the vehicle (Fig. 3). The areas of reduced pressure are found at about one third of the bodywork surface and around the wheels (Fig. 2 to 4). The highest underpressure affecting the car occurs on the outer side of the wheels, reaching a value of $-168.07[\text{Pa}]$. The presence of vacuum is connected with the principle of Bernoulli equation and the maximum air flow rate at this point, reaching a value of $13.97[\text{m/s}]$. Around the roof and the wheels of the vehicle there are visible areas of increased air flow velocity (Fig. 5 and 6). Around the "nose" and "tail" the flow rate is visibly reduced. The minimum value of $0.1[\text{m/s}]$ is obtained on the surface of the body behind the rear wheels. There is hardly any separation of the air stream on the "tail" (Fig. 7 and 8), but despite this fact some turbulence occurs at the end of the tail (Fig. 9). The strongest rotation of air molecules during the flow along the bodywork is observed in the front and at the bottom of the vehicle as well as behind the wheels (Fig. 10).

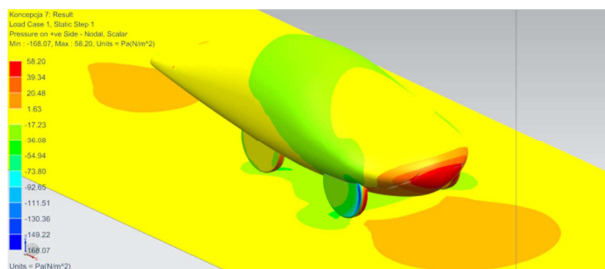


Fig.2. The pressure distribution exerted on the surface of the vehicle body for the seventh concept - trimetric view

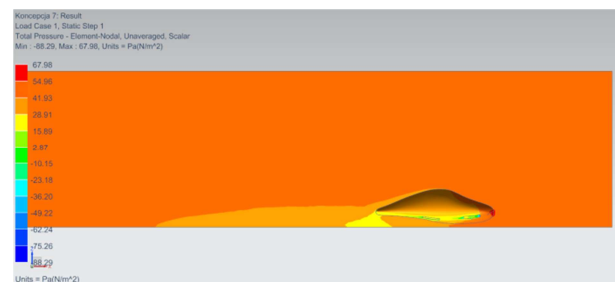


Fig.3. The pressure distribution around the vehicle body for the seventh concept - longitudinal section

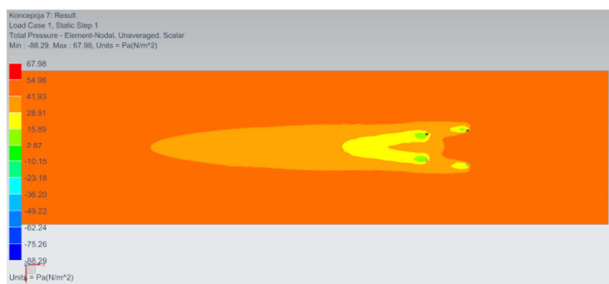


Fig.4. The pressure distribution around the vehicle body for the seventh concept - bottom view

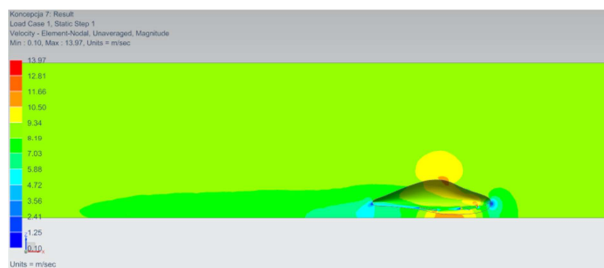


Fig.5. The velocity distribution of air flow around the vehicle body for the seventh concept - longitudinal section

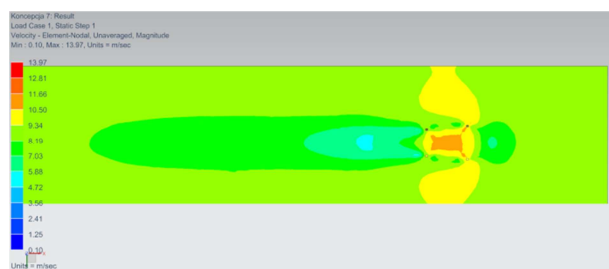


Fig.6. The velocity distribution of air flow around the vehicle body for the seventh concept - bottom view

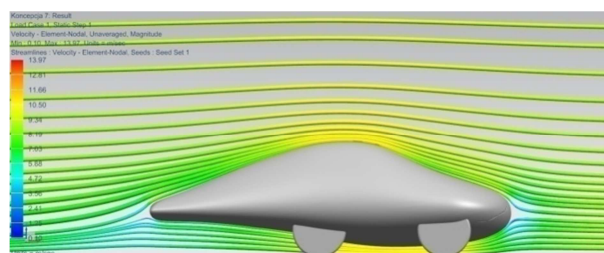


Fig.7. Flow lines around the vehicle body for the seventh concept - side view

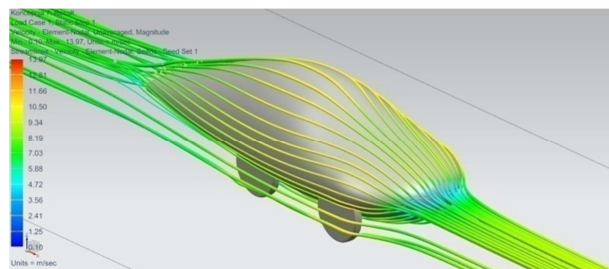


Fig.8. Flow lines around the vehicle body for the seventh concept - trimetric view

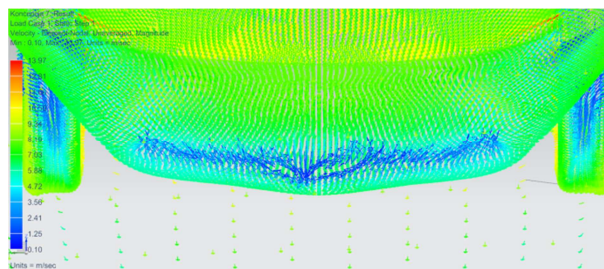


Fig.9. The presence of vortices on the "tail" of the vehicle body for the seventh concept

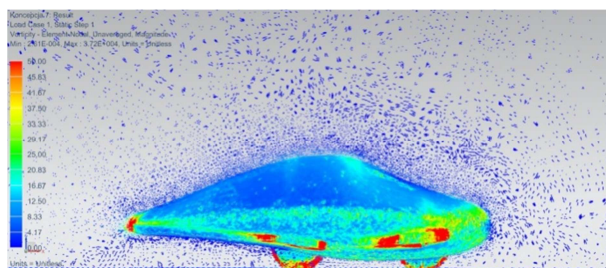


Fig.10. The rotation of air molecules during the flow along the vehicle body for the seventh concept - longitudinal section

6. Conclusion

The information collected from the conducted simulations provides a basis for further work on the bodywork with a low value of aerodynamic resistance. The drag coefficient c_x and the surface of the front area are important values of the vehicle aerodynamics but only their product translates directly into the force of air resistance. The best result of one of these values does not determine the most optimal solution in terms of air resistance force. The bodywork with the lowest value of air resistance force is not necessarily an optimal solution from the point of view of the minimum drag criterion. This force is merely one of the components and only after summing it with the lift force it is possible to receive a total aerodynamic resistance.

References

1. Shell Eco-marathon Official Rules 2013
2. Foley J.D., Dam A., Freiner S.K., Hughes J.F., Phillips R.L.: Introduction to Computer Graphics, Jan Zabrodzki (translation), WNT, Warszawa, 1995. (In Polish)
3. Gierej J.: Construction of bodyworks - guide, Lectures for students of SiMR Warsaw University of Technology, 2004 (In Polish)
4. Hucho W.H. (collective work edited by): The aerodynamics of the car: from the mechanics of flow to the vehicle build, WKiŁ, Warszawa, 1988 (In Polish)
5. Jackowski J., Łęgiewicz J., Wieczorek M.: Passenger cars and derivative, WKiŁ, Warszawa, 2011 (In Polish)
6. Katz J.: Race Car aerodynamics, Robert Bentley Automotive Publishers, 1995
7. Piechna J.: Basic aerodynamics of vehicles, WKiŁ, Warszawa, 2000 (In Polish)
8. Prochowski L.: Mechanics of motion, WKiŁ, Warszawa, 2005 (In Polish)
9. Rusiński E.: Principles of design of load-bearing structures of vehicles, The Publishing House of Wrocław University of Technology, Wrocław, 2002 (In Polish)
10. Rychter T.: Construction of vehicles, Ed. 7, WSiP, Warszawa, 1999 (In Polish)
11. Zieliński A.: The construction of bodyworks of cars and derivatives, Ed. 3, WKiŁ, Warszawa, 2008 (In Polish)
12. Zuba M.: The concept of the electric car in the Urban category, Thesis, Gliwice, 2013 (In Polish)
13. <http://www.turbmodels.larc.nasa.gov/> (dated 15.05.2013)